



Role of Marginal Seas in Deep Ocean Regeneration of Dissolved Silica: A Case Study in the Marginal Seas of the Western Pacific

Xiaoqing Yu^{1,2}, Yanpei Zhuang^{1,3*}, Xiaoxia Cai¹ and Di Qi¹

¹ Polar and Marine Research Institute, Jimei University, Xiamen, China, ² Xiamen Municipal Southern Marine Testing Center, Xiamen, China, ³ Southern Marine Science and Engineering Guangdong Laboratory (Zhuhai), Zhuhai, China

OPEN ACCESS

Edited by:

Fajin Chen,
Guangdong Ocean University, China

Reviewed by:

Dongliang Lu,
Beibu Gulf University, China
Feng Ye,
Guangzhou Institute of Geochemistry,
Chinese Academy of Sciences (CAS),
China
Weifeng Yang,
Xiamen University, China

*Correspondence:

Yanpei Zhuang
zhuangyp@jum.edu.cn

Specialty section:

This article was submitted to
Marine Biogeochemistry,
a section of the journal
Frontiers in Marine Science

Received: 22 April 2022

Accepted: 16 May 2022

Published: 15 June 2022

Citation:

Yu X, Zhuang Y, Cai X and Qi D (2022)
Role of Marginal Seas in Deep Ocean
Regeneration of Dissolved Silica: A
Case Study in the Marginal Seas of the
Western Pacific.
Front. Mar. Sci. 9:925919.
doi: 10.3389/fmars.2022.925919

Deep ocean regeneration of dissolved silica (DSi) is an essential part of the ocean silica cycle and is driven by a complex series of biogeochemical processes. Here we compare the distributions of DSi and other environmental parameters in several western Pacific marginal seas to explore the role of marginal seas in deep ocean DSi regeneration. Results show that in oligotrophic marginal seas (such as the South China Sea), the DSi content in deep waters is similar to that of the adjacent Pacific waters. However, in productive marginal seas (such as the Bering Sea), the DSi content in deep waters is markedly higher than that in adjacent Pacific waters at the same depths. This is mainly due to deep ocean DSi regeneration in the marginal sea basin, which is fueled by the high biogenic particle flux from the productive surface waters. On a global scale, deep ocean DSi regeneration is accelerated in productive marginal seas, causing marginal seas such as the Bering Sea to have the highest DSi concentrations of all global waters.

Keywords: marine Si cycle, deep waters, Bering Sea, South China Sea, marginal seas

INTRODUCTION

The present marine silica cycle appears to be near internal equilibrium, but has the dynamic interconversion of dissolved silica (DSi; also known as silicic acid) and biogenic silica (BSi; also known as opal) (Nelson et al., 1995; Ragueneau et al., 2006; Tréguer et al., 2021). BSi is produced mainly by pelagic siliceous organisms (mainly diatoms), which absorb DSi from the surface ocean to build their skeletons. They are then exported to the subsurface and deep waters under the action of the biological carbon pump (Moriceau et al., 2019). Benthic siliceous organisms (e.g., sponges) also contribute to oceanic BSi production (Maldonado et al., 2019). Global annual BSi production has recently been estimated at nearly 260 Tmol Si yr⁻¹ (Tréguer et al., 2021). Approximately two-thirds of newly synthesized BSi are redissolved in the upper 2000 m of water column, and only ~5% is permanently buried in sediment (Tréguer and de la Rocha, 2013). The remaining BSi is redissolved to form DSi in deep waters and in surface sediment, and this contributes to deep ocean DSi regeneration in the ocean interior (Heinze et al., 2003). Large amounts of deep-water DSi reach the upper ocean by upwelling and vertical mixing in certain regions, such as the Southern and North Pacific oceans (Sarmiento et al., 2004).

Marginal seas lie between the continental margin and the open ocean, are separated from the open ocean by islands or archipelagos, and are influenced by both land and open ocean (Wang, 1999). Certain marginal seas may have high diatom productivity and thus high rates of BSi formation due to the input of nutrients and biogenic matter from coastal waters (e.g., the Bering Sea; Waga et al., 2022). Conversely, some marginal seas may be as oligotrophic as the open ocean, with phytoplankton biomass dominated by picophytoplankton rather than diatoms (e.g., the South China Sea; Li et al., 2022a). These differences are closely related to differences in the oceanic CO₂ flux (Dai et al., 2013), BSi export (Cao et al., 2020), and the biological carbon pump (Li et al., 2022b) in marginal seas. A mechanistic understanding of the role of marginal seas in deep ocean DSi regeneration is critical if we are to fully understand the functioning of the marine silica cycle.

The oceanic silica flux and budget, silica balance, and major redistribution pathways are well established for the global oceans and marginal seas (DeMaster, 1981; Nelson et al., 1995; Tréguer et al., 1995; Sarmiento et al., 2004; Wu and Liu, 2020; Ma et al., 2022). However, the role of marginal seas in deep ocean DSi regeneration has not yet been discussed in detail. Here, we use available data on nutrient distributions, salinity, apparent oxygen utilization (AOU), and nutrient tracers to explore differences in DSi distributions and their controlling factors in deep waters of the western Pacific marginal sea basins. We discuss the distinct role of marginal seas in deep ocean DSi regeneration using the South China Sea, Japan Sea, Okhotsk Sea, and Bering Sea as examples.

MATERIALS AND METHODS

Nutrient, dissolved oxygen, and hydrographic data were obtained from the World Ocean Database (WOD; <https://www.ncei.noaa.gov/access/world-ocean-database/datawodgeo.html>). The study area includes the North Atlantic, Southern, Indian, and North Pacific oceans, which are open ocean waters, and the Bering Sea, Okhotsk Sea, Japan Sea, and South China Sea, which are marginal seas (**Supplementary Table 1**). Although the data acquisition time in this study was from 1981 to 2016, the deep-water DSi data are still comparable, mainly because deep-water DSi does not change over long periods of time (at least hundreds of years) (Béthoux et al., 1998; Hendry et al., 2010). For spatial visualization and analysis of the nutrient and hydrographic data, we used Ocean Data View (ODV) version 4.4.1 (Schlitzer, 2018).

Nutrient tracer Si*, with a formula of $Si^* = [DSi] - [NO_3^-]$ (Brzezinski et al., 2002; Sarmiento et al., 2004), is calculated to indicate an excess/deficit of silicate relative to nitrate. Another widely used nutrient tracer N* ($N^* = ([NO_3^-]) - 16[PO_4^{3-}] + 2.90 \mu\text{mol/kg} \times 0.87$) is calculated to determine the net effect of nitrogen fixation and denitrification (Gruber and Sarmiento, 1997). AOU is calculated as the O₂ solubility in seawater minus the measured O₂ concentration (Garcia and Gordon, 1992).

RESULTS

DSi Distribution in Global Waters

We compared the DSi distributions of deep waters (>2000 m) of the North Atlantic, Southern, Indian, and North Pacific oceans as examples of the global ocean (**Figure 1**). The North Atlantic Ocean is the starting point of the global ocean conveyor belt (**Figure 1A**) and has the lowest deep-water DSi concentration ($29.0 \pm 12.1 \mu\text{mol/kg}$) in the global ocean (**Figure 1B**). The average concentration of DSi in deep waters of the Southern Ocean is $111.0 \pm 12.5 \mu\text{mol/kg}$. The average deep-water DSi concentration in the Indian Ocean is $124.3 \pm 4.5 \mu\text{mol/kg}$, which is slightly higher than that in the Southern Ocean and nearly 95 $\mu\text{mol/kg}$ higher than the average deep-water DSi concentration in the North Atlantic. The North Pacific is located at the end of the deep current in the global ocean conveyor belt (**Figure 1A**). The average deep-water concentration of DSi in the North Pacific is $157.7 \pm 5.7 \mu\text{mol/kg}$, which is nearly 129 and 34 $\mu\text{mol/kg}$ higher than the average concentrations in the North Atlantic and Southern oceans, respectively. These results suggest that DSi accumulates during the transport of deep currents through the global ocean conveyor belt.

Deep-water DSi concentrations in the North Atlantic increase with increasing water depth (**Figure 1B**). The average DSi concentration at 2000-m water depth is $11.7 \pm 0.8 \mu\text{mol/kg}$, which increases to $22.2 \pm 1.9 \mu\text{mol/kg}$ at 3000 m, and then to $43.9 \pm 1.1 \mu\text{mol/kg}$ at 4000 m. Similarly, data from the Southern Ocean, another major region of deep-water formation, show an increase in DSi content with depth in deep waters. The average DSi concentration at a depth of 2000 m in the Southern Ocean is $86.3 \pm 2.8 \mu\text{mol/kg}$, and this increases to $124.0 \pm 0.8 \mu\text{mol/kg}$ at a depth of 4000 m. In contrast, there are no increases in DSi content with depth in deep waters of the Indian and North Pacific oceans.

The regeneration of DSi (or dissolution of BSi) occurs concurrently with respiration of organic matter. Vertical profiles of nitrate concentrations typically show their highest values at depths of 500–1000 m (**Figure 1C**), coinciding with the depths at which rates of respiration are also at their highest (as indicated by AOU maxima, **Supplementary Figure S1A**) in the open oceans. Deep-water nitrate concentrations may decrease with increasing water depth owing to the removal of nitrogen during denitrification (as indicated by negative N* values, **Supplementary Figure S1B**). However, nitrate concentrations increase with depth in the deep-water layers (>2000 m) of the North Atlantic and Southern Ocean (**Figure 1C**). These results suggest high rates of organic matter remineralization and DSi regeneration in deep waters of the North Atlantic and Southern oceans, which may be associated with sinking biogenic particles during the formation of deep waters.

Deep-Water DSi Distribution in Marginal Seas

We compared deep-water DSi concentrations among the marginal seas of the western Pacific (the Bering Sea, Okhotsk Sea, Japan Sea, and South China Sea) and with the DSi

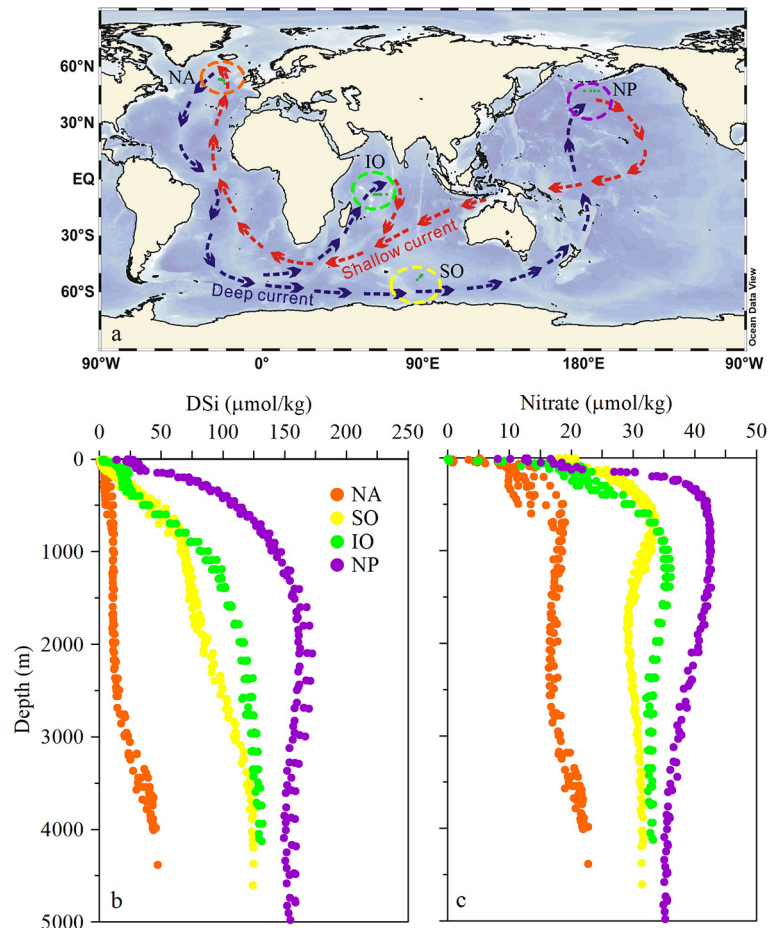


FIGURE 1 | Distribution of DSi and nitrate concentrations ($\mu\text{mol/kg}$) in the open oceans at different stages of the global ocean conveyor belt. **(A)** Schematic map of the global ocean conveyor belt (after Lozier, 2010); blue and red arrows indicate deep and shallow currents, respectively. Vertical distributions of **(B)** DSi and **(C)** nitrate concentrations in the study areas in the North Atlantic (NA), Southern (SO), Indian (IO), and North Pacific (NP) oceans.

concentrations of the adjacent Pacific waters for reference. There are three distinct patterns of deep-water DSi distribution in the marginal seas, with DSi concentrations either being higher, lower, or equal to the average of the adjacent Pacific waters (**Figure 2**). The average DSi concentration in deep waters of the Bering Sea is $212.6 \pm 11.8 \mu\text{mol/kg}$, which is $\sim 50 \mu\text{mol/kg}$ higher than that in the adjacent deep Pacific Ocean ($159.1 \pm 6.5 \mu\text{mol/kg}$). The deep-water DSi concentration in the Okhotsk Sea is slightly higher than that in the adjacent Pacific waters, with an average of $170.4 \pm 2.6 \mu\text{mol/kg}$. In contrast, the deep-water DSi concentration in the Japan Sea is far lower than that in the adjacent Pacific water, with an average value of only $80.1 \pm 3.3 \mu\text{mol/kg}$. The average DSi concentration in deep waters of the South China Sea is $151.4 \pm 4.6 \mu\text{mol/kg}$, which is close to the average DSi concentration of the adjacent Pacific waters ($142.9 \pm 2.0 \mu\text{mol/kg}$).

The different patterns of deep-water DSi distribution in the marginal seas may be related to the effects of intrusion of deep currents from the Pacific Ocean on their deep waters. This is important because deep currents in the Pacific Ocean have

accumulated large amounts of DSi along the global ocean conveyor belt. For example, the Japan Sea, which is only connected to the open ocean through a shallow waterway, does not receive large amounts of DSi-rich Pacific deep waters; therefore, the deep-water DSi reserve in the Japan Sea depends mainly on its internal silica cycle. This is supported by deep-water salinity distributions in the Japan Sea, which are markedly different from those in adjacent Pacific waters, whereas the other marginal seas show very similar salinity distributions to their adjacent Pacific waters (**Supplementary Figure S2**). In marginal seas where the main ocean current is derived directly from the open ocean, such as in the Bering Sea, the Okhotsk Sea, and the South China Sea, the deep-water DSi concentrations are equal to or higher than those of the inflowing Pacific Ocean waters.

The mean deep-water DSi concentration in the Bering Sea is $50 \mu\text{mol/kg}$ higher than that in the adjacent Pacific waters. This indicates that deep-water DSi distributions in the marginal seas are closely linked to deep DSi regeneration. We calculated deep-water DSi regeneration as the difference in DSi concentration between the seafloor and 2000-m depth in the water column

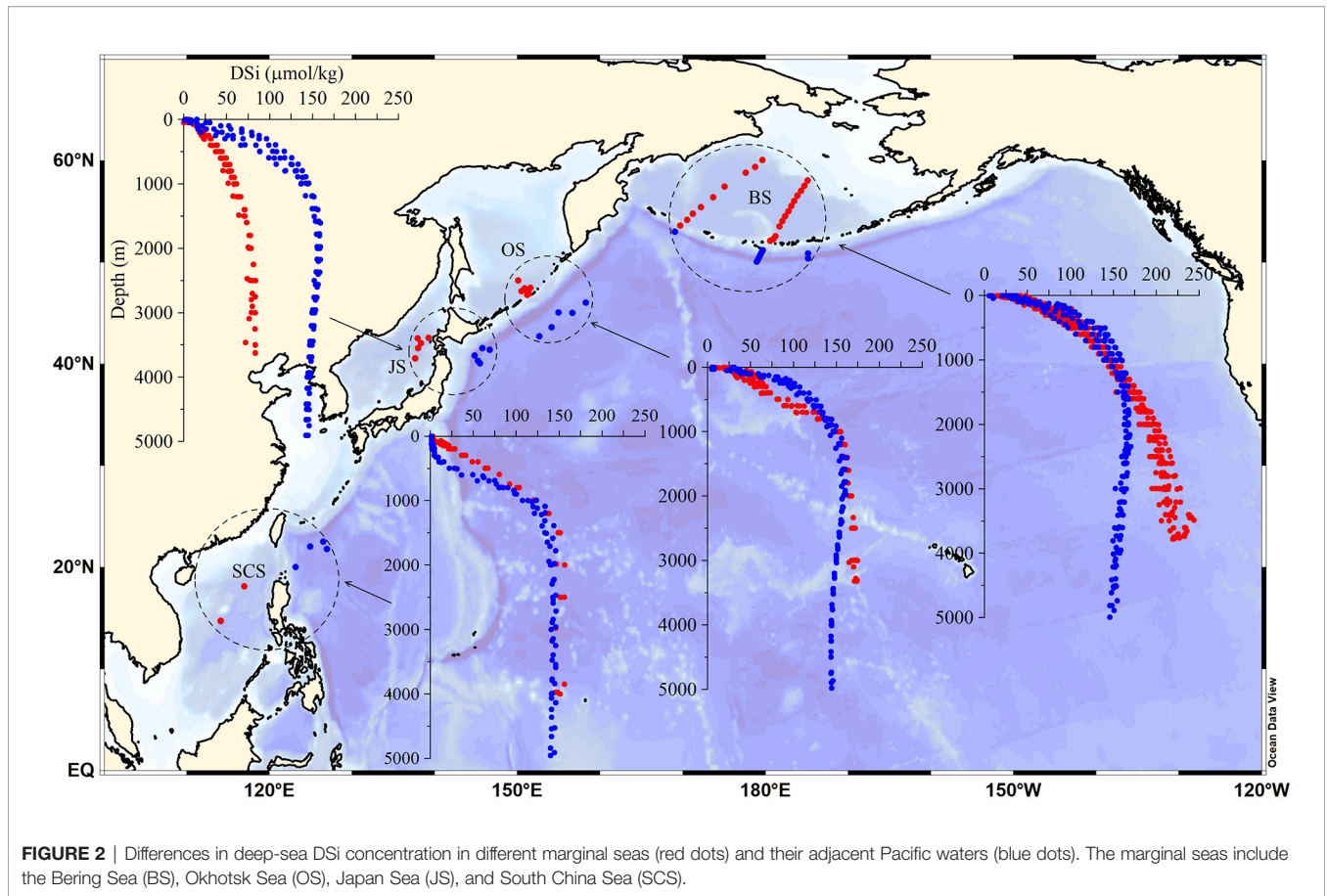


FIGURE 2 | Differences in deep-sea DSi concentration in different marginal seas (red dots) and their adjacent Pacific waters (blue dots). The marginal seas include the Bering Sea (BS), Okhotsk Sea (OS), Japan Sea (JS), and South China Sea (SCS).

($\Delta\text{DSi}_{(\text{bottom}-2000\text{m})}$, $\mu\text{mol/kg}$). The $\Delta\text{DSi}_{(\text{bottom}-2000\text{m})}$ value in the Bering Sea is $32.8 \pm 4.0 \mu\text{mol/kg}$ (Figure 3), whereas the $\Delta\text{DSi}_{(\text{bottom}-2000\text{m})}$ values in the Okhotsk Sea, Japan Sea, and South China Sea are 5.8 ± 2.6 , 3.1 ± 2.5 , and $-0.5 \pm 0.7 \mu\text{mol/kg}$,

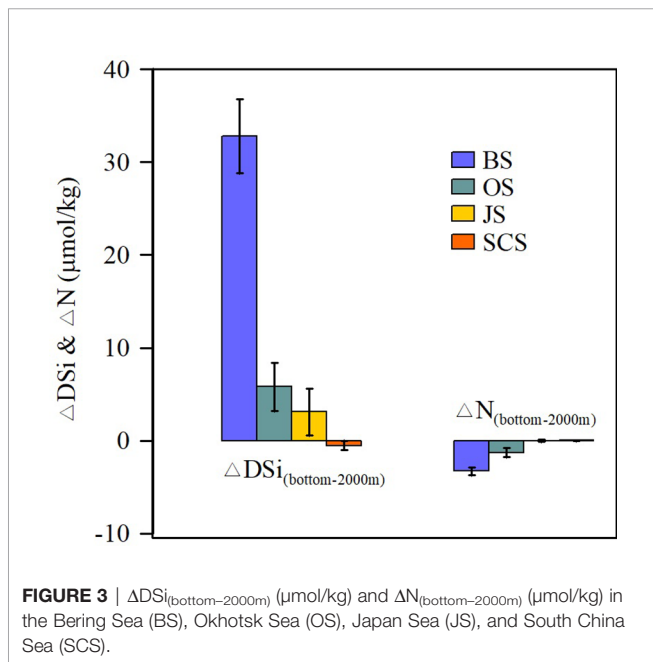


FIGURE 3 | $\Delta\text{DSi}_{(\text{bottom}-2000\text{m})}$ ($\mu\text{mol/kg}$) and $\Delta\text{N}_{(\text{bottom}-2000\text{m})}$ ($\mu\text{mol/kg}$) in the Bering Sea (BS), Okhotsk Sea (OS), Japan Sea (JS), and South China Sea (SCS).

respectively. $\Delta\text{N}_{(\text{bottom}-2000\text{m})}$ is negative or close to 0 in the marginal seas, indicating nitrogen removal by denitrification. The Bering Sea show similar deep-water salinity distributions to the adjacent Pacific waters (Supplementary Figure S2), suggesting the influence of deep currents intrusion from the Pacific Ocean. However, no strong nitrate removal was observed in the deep North Pacific. These results indicate strong DSi regeneration in deep waters of the Bering Sea, accompanied by active nitrate removal.

Deep-Water DSi Distribution in the Bering Sea

As shown in Figure 4, the DSi distribution at shallow depths (<1000 m) in the Bering Sea is similar to that in the North Pacific. However, DSi concentrations in deep waters of the Bering Sea are markedly higher than those in the North Pacific, indicating high rates of DSi regeneration in the former (Figure 4A). DSi concentrations in the Bering Sea increase with water depth, and high silica concentrations (>225 $\mu\text{mol/kg}$) are observed in the near-bottom waters of the northern basin. DSi concentrations are as high as 241.4 $\mu\text{mol/kg}$, which means the deep waters of the Bering Sea have the highest reported DSi concentrations of the global ocean.

Microbial respiration of sinking biogenic detritus leads to the formation of AOU maxima (>300 $\mu\text{mol/kg}$) at depths between 300 and 1200 m in the North Pacific (Figure 4B). The layer

where $\text{AOU} > 300 \mu\text{mol/kg}$ deepens to 1600 m in the Bering Sea (**Figure 4B**). As is the case with DSi, the deep-water concentrations of AOU in the Bering Sea are markedly higher than those in the North Pacific (**Figure 4B**), indicating high rates of organic matter remineralization in deep waters of the Bering Sea. However, nitrate concentrations in the deep waters of the Bering Sea are comparable to those in the Pacific Ocean (**Supplementary Figure S3A**); this may be due to nitrogen loss through intensive denitrification, as evidenced by the negative deep-water N^* values in the Bering Sea (**Figure 4C**). Conversely, Si^* values in the Bering Sea are extremely high, with an average Si^* value of $174.8 \pm 12.8 \mu\text{mol/kg}$ (**Supplementary Figure S3B**). These results suggest an active biogeochemical cycle and the rapid accumulation of DSi in deep waters of the Bering Sea.

DISCUSSION

The results indicate that deep-water (>2000 m) DSi reserves in the marginal seas of the western Pacific Ocean are first related to the extent to which they connect and exchange with the open ocean. When the main current of the marginal sea is derived from the open ocean (**Figures 5A, B**), such as in the Bering Sea,

the Okhotsk Sea, and the South China Sea, the deep water receives a high DSi input from the open ocean, and the DSi concentrations are equal to or higher than those of the adjacent Pacific deep waters. The deep-water DSi concentration in the Bering Sea (average of $212.6 \pm 11.8 \mu\text{mol/kg}$) is $\sim 50 \mu\text{mol/kg}$ higher than that in the adjacent deep Pacific Ocean. When there is limited connectivity between the marginal sea and the open ocean (e.g., the waterway is shallower than 100 m), deep waters in the marginal sea are not markedly affected by inputs from the adjacent ocean deep water and deep-water DSi concentrations are lower than those in the adjacent open ocean (**Figure 5C**), as observed for the Japan Sea. The deep-water DSi concentration in the Japan Sea (average of $80.1 \pm 3.3 \mu\text{mol/kg}$) is $\sim 70 \mu\text{mol/kg}$ lower than that in the adjacent Pacific water. The deep-water DSi reserves of marginal seas are also strongly influenced by internal DSi regeneration. Higher rates of deep ocean DSi regeneration will lead to higher DSi concentrations in the deep waters of marginal seas than in the adjacent Pacific Ocean, as is the case in the Okhotsk Sea and the Bering Sea (**Figure 5B**).

The role of marginal seas in deep ocean DSi regeneration is tightly coupled with the formation of BSi *via* diatom production in the surface waters. The South China Sea, the largest marginal sea in the Pacific Ocean, has a very active biogeochemical cycle in

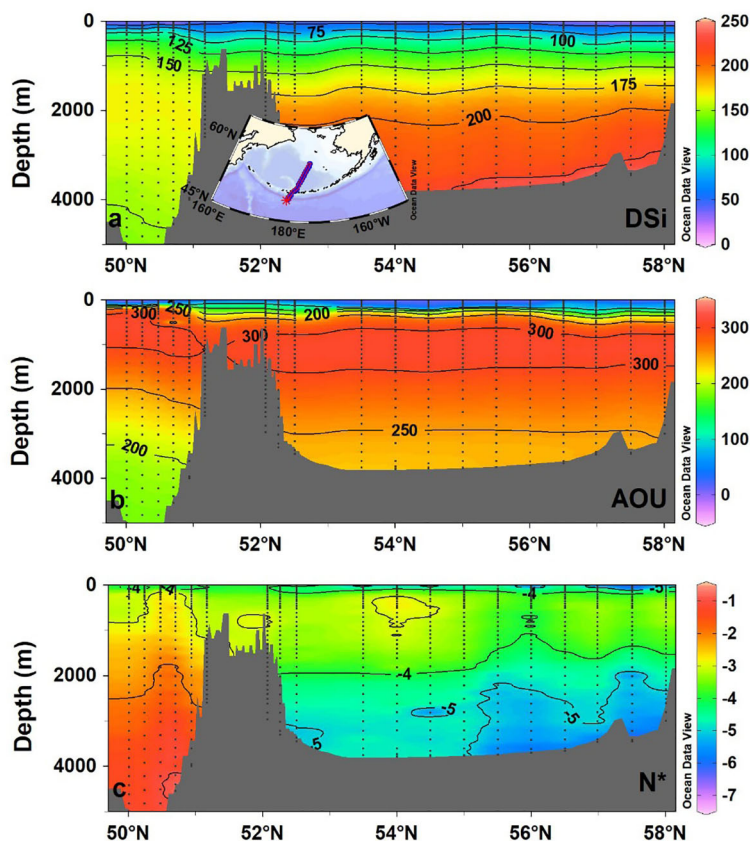


FIGURE 4 | Cross-sectional distribution of (A) DSi ($\mu\text{mol/kg}$), (B) apparent oxygen utilization (AOU; $\mu\text{mol/kg}$), and (C) N^* ($\mu\text{mol/kg}$) in the North Pacific Ocean and Bering Sea. The nutrient tracer N^* represents the net effect of nitrogen fixation and denitrification.

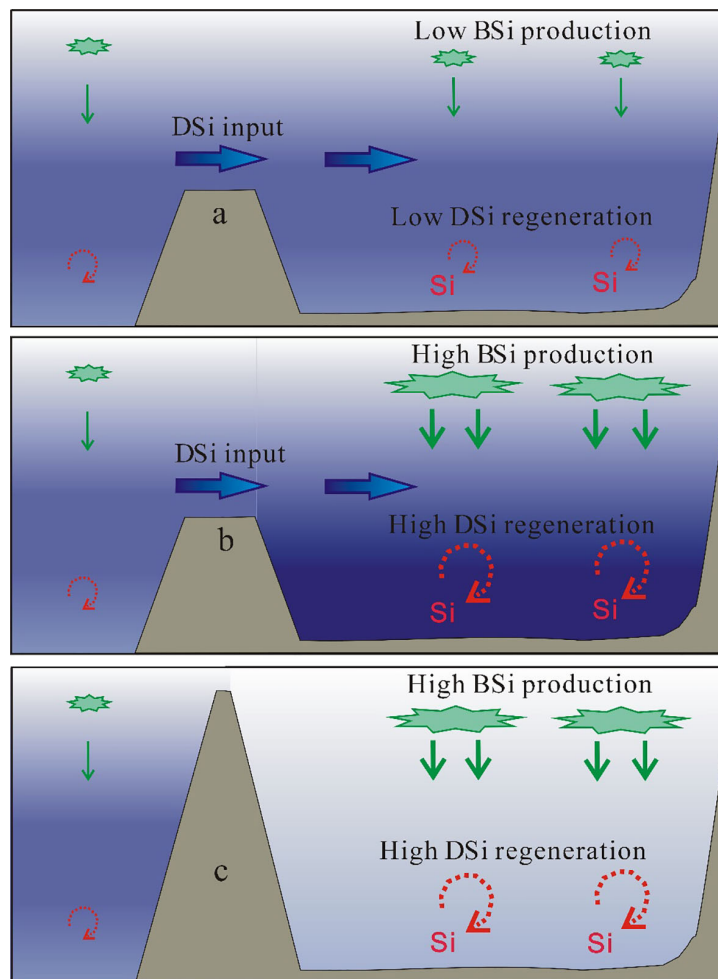


FIGURE 5 | Schematic diagrams showing the silica cycle in different marginal sea settings. **(A)** Oligotrophic marginal sea under the influence of open ocean inflow water; **(B)** productive marginal sea under the influence of open ocean inflow water; **(C)** marginal sea unaffected by open ocean inflow water. The background color indicates the concentration of DSi, with darker colors indicating higher concentrations.

its adjacent coastal waters (e.g., Cao et al., 2012; Lu et al., 2022). However, it is nutrient-poor in the mid-ocean, especially in anticyclonic eddies (Du et al., 2013; Zhuang et al., 2018; Sun et al., 2022), where persistent stratification limits the vertical influx of nutrients (Wong et al., 2007; Zhuang et al., 2021a). Here, the supply of nutrients to surface layers (and the subsequent increase in particles sinking to depth) depends on episodic events such as typhoons (Zhang et al., 2019; Chen et al., 2021). The monthly mean BSi flux in the central South China Sea ranges from 14.8 to 34.9 $\text{mg m}^{-2} \text{d}^{-1}$, with a high BSi flux during the northeastern monsoon period (Li et al., 2017). When the surface waters of marginal seas are oligotrophic, as in the South China Sea, the rates of formation and export of BSi are low (Yang et al., 2015), which leads to low rates of DSi regeneration of in deep waters (**Figure 5A**). It has been indicated that oligotrophic areas have low rates of BSi dissolution and benthic diffusion of DSi (Tréguer et al., 1995). Deep ocean DSi regeneration is more intense when the surface waters of marginal seas are productive

(**Figure 5B**), such as in the Bering Sea and the Okhotsk Sea. The monthly mean BSi flux in the southern Bering Sea ranges from 48.4 to 805.0 $\text{mg m}^{-2} \text{d}^{-1}$ (Akagi et al., 2011), which is an order of magnitude higher than that in the South China Sea (14.8 to 34.9 $\text{mg m}^{-2} \text{d}^{-1}$; Li et al., 2017). The strong particle flux through the water column in the productive marginal seas promotes the sinking of BSi to deep waters and sediment.

Other physical and biogeochemical factors also contribute to the high rates of deep ocean DSi regeneration in the Bering Sea. First, a summertime high-productivity zone, also known as the “green belt”, exists along the shelf break of the Bering Sea and is maintained by upward influx of nutrients and iron from the subsurface (Springer et al., 1996; Tanaka et al., 2012). The phytoplankton community in the region is dominated by diatoms, which contribute to high biological production and thus high rates of BSi formation (Zhuang et al., 2020). Second, there are mechanisms that lead to the rapid sinking of biogenic particles in this area. For example, oceanic deep-water formation

in the Atlantic and Southern oceans leads to the rapid removal of additional particles from the surface by water mass subduction (Lohmann et al., 2006). Low surface temperatures in the subpolar Bering Sea favor BSi preservation, which results in reduced rates of respiration and silica dissolution in the upper ocean (Nelson et al., 1995; Iversen and Ploug, 2013). In contrast, high surface temperatures often promote the dissolution of BSi in the low-latitude oceans, such as the Japan Sea and the South China Sea. In addition, diatom-derived particles typically have lower decay rates (Cabrera-Brufau et al., 2021), which allows more biogenic particles to reach deep waters and sediment. AOU concentrations and $\Delta\text{DSi}_{(\text{bottom}-2000\text{m})}$ values in deep waters of the Bering Sea (**Figure 3**) indicate concurrent organic matter remineralization and BSi dissolution as biogenic particles sink through deep waters. The amount of DSI regeneration varies throughout the global oceans, mostly because of differences in the rates of organic matter remineralization (Guidi et al., 2015). Hu et al. (2014) showed that the Bering Sea has an extremely high particle removal rate, which may be one of the main reasons for the high rates of DSI release in deep waters of the Bering Sea.

The Bering Sea experienced high rates of BSi export production, equal to those in the Southern and eastern equatorial Pacific oceans, but BSi concentrations in Bering Sea sediments are relatively low (Heinze et al., 2003). This strongly suggests that deep ocean DSI regeneration in the Bering Sea is accelerated relative to that in the open ocean. Earlier works have alluded to higher BSi recycling fluxes under low oxygen conditions (Berelson et al., 1987) and a decrease in BSi preservation under anoxic waters (Dale et al., 2021), suggesting a dependence of BSi preservation on oxygen levels. The deep waters of the Bering Sea have high rates of organic matter respiration and thus oxygen consumption, leading to low oxygen concentrations. These low oxygen conditions may also promote DSI regeneration. In addition, the high DSI concentrations ($>225 \mu\text{mol/kg}$) observed in the near-bottom waters of the Bering Sea basin (**Figure 4**) were most likely generated locally through dissolution of BSi in surface sediments. An average sedimentary denitrification rate of nearly $230 \mu\text{mol N m}^{-2} \text{d}^{-1}$ has been reported in the deep Bering Sea ($>2000 \text{ m}$); this value is three times higher than the global average for the same depth (Lehmann et al., 2005). DSI is released into deep waters at the sediment–water interface, which increases the deep-water DSI reserves. Active benthic biogeochemical processes may also contribute to deep ocean DSI regeneration in the Bering Sea. The high regeneration rate of deep ocean DSI and upwelling water will eventually affect the regional nutrient budget and cycle (Zhuang et al., 2021b).

CONCLUSIONS

The role of marginal seas in deep ocean DSI regeneration is tightly coupled to the production and export of BSi in surface waters. In the nutrient-poor South China Sea, the deep-water DSI concentration is close to that of the adjacent Pacific waters, and deep ocean DSI regeneration is weak. Conversely, in the productive Bering Sea, deep-water DSI concentrations are much higher than those in the adjacent

Pacific waters, and the capacity for deep DSI regeneration is strong; as a result, the Bering Sea has the highest reported deep-water DSI concentrations ($>240 \mu\text{mol/kg}$) in the global ocean. A combination of physical and biochemical factors, including low temperatures, diatom-dominance in the phytoplankton community, high particle export rate, and dissolution of opal in surface sediments, contribute to active DSI regeneration in deep waters of the Bering Sea.

Although marginal seas represent only a small fraction of the global ocean area, and the rapid accumulation of DSI in the deep waters of marginal seas may not seem globally significant, they may have important regional implications. Deep ocean DSI regeneration and organic matter respiration are accelerated in productive marginal seas, suggesting active deep ocean biogeochemical cycles in these regions and may support unexpectedly active ecosystem (e.g., bacteria) in the deep water and sediments. Besides, the upwelling water of the Bering Sea and its northward flow have important effects on the nutrient budget and ecosystem of the adjacent Arctic Ocean.

DATA AVAILABILITY STATEMENT

Publicly available datasets were analyzed in this study. This data can be found here: <https://www.ncei.noaa.gov/access/world-ocean-database/datawodgeo.html>.

AUTHOR CONTRIBUTIONS

Conceptualization, XY and YZ. methodology and software, XY and XC. Validation, XY and YZ. Data curation, XY and YZ. Writing—original draft preparation, XY. Writing—review and editing, YZ, XC, and DQ. Supervision and project administration, YZ. Funding acquisition, YZ and DQ. All authors have read and agreed to the published version of the manuscript.

FUNDING

This research was funded by National Key Research and Development Program of China (2019YFE0120900, and 2019YFE0114800), the Natural Science Foundation of Zhejiang Province (Y19D060024).

ACKNOWLEDGMENTS

We thank the World Ocean Database (<https://www.ncei.noaa.gov/access/world-ocean-database/datawodgeo.html>) for provision of the data.

SUPPLEMENTARY MATERIAL

The Supplementary Material for this article can be found online at: <https://www.frontiersin.org/articles/10.3389/fmars.2022.925919/full#supplementary-material>

REFERENCES

- Akagi, T., Fu, F. F., Hongo, Y., and Takahashi, K. (2011). Composition of Rare Earth Elements in Settling Particles Collected in the Highly Productive North Pacific Ocean and Bering Sea: Implications for Siliceous-Matter Dissolution Kinetics and Formation of Two REE-Enriched Phases. *Geochim. Cosmochim. Ac.* 75 (17), 4857–4876. doi: 10.1016/j.gca.2011.06.001
- Berelson, W. M., Hammond, D. E., and Johnson, K. S. (1987). Benthic Fluxes and the Cycling of Biogenic Silica and Carbon in Two Southern California Borderland Basins. *Geochim. Cosmochim. Ac.* 51 (6), 1345–1363. doi: 10.1016/0016-7037(87)90320-6
- Béthoux, J. P., Morin, P., Chaumery, C., Connan, O., Gentili, B., and Ruiz-Pino, D. (1998). Nutrients in the Mediterranean Sea, Mass Balance and Statistical Analysis of Concentrations With Respect to Environmental Change. *Mar. Chem.* 63 (1–2), 155–169. doi: 10.1016/S0304-4203(98)00059-0
- Brzezinski, M. A., Pride, C. J., Franck, V. M., Sigman, D. M., Sarmiento, J. L., Matsumoto, K., et al. (2002). A Switch From Si(OH)₄ to NO₃⁻ Depletion in the Glacial Southern Ocean. *Geophys. Res. Lett.* 29 (12), 1564. doi: 10.1029/2001GL014349
- Cabrera-Brufau, M., Arin, L., Sala, M. M., Cermeño, P., and Marrasé, C. (2021). Diatom Dominance Enhances Resistance of Phytoplanktonic POM to Mesopelagic Microbial Decomposition. *Front. Mar. Sci.* 8. doi: 10.3389/fmars.2021.683354
- Cao, Z., Frank, M., Dai, M., Grasse, P., and Ehlert, C. (2012). Silicon Isotope Constraints on Sources and Utilization of Silicic Acid in the Northern South China Sea. *Geochim. Cosmochim. Ac.* 97, 88–104. doi: 10.1016/j.gca.2012.08.039
- Cao, Z., Wang, D., Zhang, Z., Zhou, K., Liu, X., Wang, L., et al. (2020). Seasonal Dynamics and Export of Biogenic Silica in the Upper Water Column of a Large Marginal Sea, the Northern South China Sea. *Prog. Oceanogr.* 188, 102421. doi: 10.1016/j.pcean.2020.102421
- Chen, F., Huang, C., Lao, Q., Zhang, S., Chen, C., Zhou, X., et al. (2021). Typhoon Control of Precipitation Dual Isotopes in Southern China and its Palaeoenvironmental Implications. *J. Geophys. Res.* 126 (14), e2020JD034336. doi: 10.1029/2020JD034336
- Dai, M., Cao, Z., Guo, X., Zhai, W., Liu, Z., Yin, Z., et al. (2013). Why are Some Marginal Seas Sources of Atmospheric CO₂? *Geophys. Res. Lett.* 40 (10), 2154–2158. doi: 10.1002/grl.50390
- Dale, A. W., Paul, K. M., Clemens, D., Scholz, F., Schroller-Lomnitz, U., Wallmann, K., et al. (2021). Recycling and Burial of Biogenic Silica in an Open Margin Oxygen Minimum Zone. *Global Biogeochem. Cy.* 35 (2), e2020GB006583. doi: 10.1029/2020GB006583
- DeMaster, D. J. (1981). The Supply and Accumulation of Silica in the Marine Environment. *Geochim. Cosmochim. Ac.* 45 (10), 1715–1732. doi: 10.1016/0016-7037(81)90006-5
- Du, C., Liu, Z., Dai, M., Kao, S. J., Cao, Z., Zhang, Y., et al. (2013). Impact of the Kuroshio Intrusion on the Nutrient Inventory in the Upper Northern South China Sea: Insights From an Isopycnal Mixing Model. *Biogeosciences* 10 (10), 6419–6432. doi: 10.5194/bg-10-6419-2013
- Garcia, H., and Gordon, L. I. (1992). Solubility of Oxygen at Different Temperature and Salinity. *Limnol. Oceanogr.* 37, 1307–1312. doi: 10.4319/lo.1992.37.6.1307
- Gruber, N., and Sarmiento, J. L. (1997). Global Patterns of Marine Nitrogen Fixation and Denitrification. *Global Biogeochem. Cy.* 11 (2), 235–266. doi: 10.1029/97GB00077
- Guidi, L., Legendre, L., Reygondeau, G., Uitz, J., Stemann, L., and Henson, S. A. (2015). A New Look at Ocean Carbon Remineralization for Estimating Deepwater Sequestration. *Global Biogeochem. Cy.* 29 (7), 1044–1059. doi: 10.1002/2014GB005063
- Heinze, C., Hupe, A., Maier-Reimer, E., Dittert, N., and Ragueneau, O. (2003). Sensitivity of the Marine Biogenic Si Cycle for Biogeochemical Parameter Variations. *Global Biogeochem. Cy.* 17 (3), 1086. doi: 10.1029/2002GB001943
- Hendry, K. R., Georg, R. B., Rickaby, R. E., Robinson, L. F., and Halliday, A. N. (2010). Deep Ocean Nutrients During the Last Glacial Maximum Deduced From Sponge Silicon Isotopic Compositions. *Earth Planet. Sci. Lett.* 292 (3–4), 290–300. doi: 10.1016/j.epsl.2010.02.005
- Hu, W., Chen, M., Yang, W., Zhang, R., Qiu, Y., and Zheng, M. (2014). Enhanced Particle Scavenging in Deep Water of the Aleutian Basin Revealed by 210Po-210Pb Disequilibria. *J. Geophys. Res.* 119 (6), 3235–3248. doi: 10.1002/2014JC009819
- Iversen, M. H., and Ploug, H. (2013). Temperature Effects on Carbon-Specific Respiration Rate and Sinking Velocity of Diatom Aggregates-Potential Implications for Deep Ocean Export Processes. *Biogeosciences* 10, 4073–4085. doi: 10.5194/bg-10-4073-2013
- Lehmann, M. F., Sigman, D. M., McCorkle, D. C., Brunelle, B. G., Hoffmann, S., Kienast, M., et al. (2005). Origin of the Deep Bering Sea Nitrate Deficit: Constraints From the Nitrogen and Oxygen Isotopic Composition of Water Column Nitrate and Benthic Nitrate Fluxes. *Global Biogeochem. Cy.* 19, GB4005. doi: 10.1029/2005GB002508
- Li, C., Chiang, K. P., Laws, E. A., Liu, X., Chen, J., Huang, Y., et al. (2022a). Quasi-Antiphase Diel Patterns of Abundance and Cell Size/Biomass of Picophytoplankton in the Oligotrophic Ocean. *Geophys. Res. Lett.* 49, e2022GL097753. doi: 10.1029/2022GL097753
- Li, H., Wiesner, M. G., Chen, J., Ling, Z., Zhang, J., and Ran, L. (2017). Long-Term Variation of Mesopelagic Biogenic Flux in the Central South China Sea: Impact of Monsoonal Seasonality and Mesoscale Eddy. *Deep-Sea. Res. Pt. I.* 126, 62–72. doi: 10.1016/j.dsr.2017.05.012
- Li, H., Zhang, J., Xuan, J., Wu, Z., Ran, L., Wiesner, M. G., et al. (2022b). Asymmetric Response of the Biological Carbon Pump to the ENSO in the South China Sea. *Geophys. Res. Lett.* 49 (2), e2021GL095254. doi: 10.1029/2021GL095254
- Lohmann, R., Jurado, E., Pilson, M. E., and Dachs, J. (2006). Oceanic Deep Water Formation as a Sink of Persistent Organic Pollutants. *Geophys. Res. Lett.* 33, L12607. doi: 10.1029/2006GL025953
- Lozier, M. S. (2010). Deconstructing the Conveyor Belt. *Science* 328 (5985), 1507–1511. doi: 10.1126/science.118925
- Lu, X., Zhou, X., Jin, G., Chen, F., Zhang, S., Li, Z., et al. (2022). Biological Impact of Typhoon Wipha in the Coastal Area of Western Guangdong: A Comparative Field Observation Perspective. *J. Geophys. Res.* 127 (2), e2021JG006589. doi: 10.1029/2021JG006589
- Maldonado, M., López-Acosta, M., Sitjà, C., García-Puig, M., Galobart, C., Errilla, G., et al. (2019). Sponge Skeletons as an Important Sink of Silicon in the Global Oceans. *Nat. Geosci.* 12 (10), 815–822. doi: 10.1038/s41561-019-0430-7
- Ma, Y., Zhang, L., Liu, S., and Zhu, D. (2022). Silicon Balance in the South China Sea. *Biogeochemistry* 157, 327–353. doi: 10.1007/s10533-021-00879-4
- Moriceau, B., Gehlen, M., Tréguer, P., Baines, S., Livage, J., and André, L. (2019). Biogeochemistry and Genomics of Silicification and Silicifiers. *Front. Mar. Sci.* 6. doi: 10.3389/fmars.2019.00057
- Nelson, D. M., Tréguer, P., Brzezinski, M. A., Leynaert, A., and Quéguiner, B. (1995). Production and Dissolution of Biogenic Silica in the Ocean: Revised Global Estimates, Comparison With Regional Data and Relationship to Biogenic Sedimentation. *Global Biogeochem. Cy.* 9 (3), 359–372. doi: 10.1029/95GB01070
- Ragueneau, O., Schultes, S., Bidle, K., Claquin, P., and Moriceau, B. (2006). Si and C Interactions in the World Ocean: Importance of Ecological Processes and Implications for the Role of Diatoms in the Biological Pump. *Global Biogeochem. Cy.* 20, GB4S02. doi: 10.1029/2006GB002688
- Sarmiento, J. L., Gruber, N., Brzezinski, M. A., and Dunne, J. P. (2004). High-Latitude Controls of Thermocline Nutrients and Low Latitude Biological Productivity. *Nature* 427 (6969), 56–60.
- Schlitzer, R. (2018). Ocean Data View. *adv.awi.de*. v.4.6.4., 2018.
- Springer, A. M., McRoy, C. P., and Flint, M. V. (1996). The Bering Sea Green Belt: Shelf-Edge Processes and Ecosystem Production. *Fish. Oceanogr.* 5 (3–4), 205–223. doi: 10.1111/j.1365-2419.1996.tb00118.x
- Sun, F., Xia, X., Simon, M., Wang, Y., Zhao, H., Sun, C., et al. (2022). Anticyclonic Eddy Driving Significant Changes in Prokaryotic and Eukaryotic Communities in the South China Sea. *Front. Mar. Sci.* 9. doi: 10.3389/fmars.2022.773548
- Tanaka, T., Yasuda, I., Kuma, K., and Nishioka, J. (2012). Vertical Turbulent Iron Flux Sustains the Green Belt Along the Shelf Break in the Southeastern Bering Sea. *Geophys. Res. Lett.* 39, L08603. doi: 10.1029/2012GL051164
- Tréguer, P. J., and de la Rocha, C. L. (2013). The World Ocean Silica Cycle. *Annu. Rev. Mar. Sci.* 5, 477–501. doi: 10.1146/annurev-marine-121211-172346
- Tréguer, P., Nelson, D. M., Van Bennekom, A. J., DeMaster, D. J., Leynaert, A., and Quéguiner, B. (1995). The Silica Balance in the World Ocean: A Reestimate. *Science* 268 (5209), 375–379. doi: 10.1126/science.268.5209.375

- Tréguer, P. J., Sutton, J. N., Brzezinski, M., Charette, M. A., Devries, T., Dutkiewicz, S., et al. (2021). Reviews and syntheses: The biogeochemical cycle of silicon in the modern ocean. *Biogeosciences*, 18 (4), 1269–1289.
- Waga, H., Fujiwara, A., Hirawake, T., Suzuki, K., Yoshida, K., Abe, H., et al. (2022). Primary Productivity and Phytoplankton Community Structure in Surface Waters of the Western Subarctic Pacific and the Bering Sea During Summer With Reference to Bloom Stages. *Prog. Oceanogr.* 201, 102738. doi: 10.1016/j.pocean.2021.102738
- Wang, P. (1999). Response of Western Pacific Marginal Seas to Glacial Cycles: Paleooceanographic and Sedimentological Features. *Mar. Geol.* 156 (1–4), 5–39. doi: 10.1016/S0025-3227(98)00172-8
- Wong, G. T., Ku, T. L., Mulholland, M., Tseng, C. M., and Wang, D. P. (2007). The SouthEast Asian Time-Series Study (SEATS) and the Biogeochemistry of the South China Sea—an Overview. *Deep-Sea. Res. Pt. II.* 54 (14–15), 1434–1447. doi: 10.1016/j.dsr2.2007.05.012
- Wu, B., and Liu, S. (2020). Dissolution Kinetics of Biogenic Silica and the Recalculated Silicon Balance of the East China Sea. *Sci. Total. Environ.* 743, 140552. doi: 10.1016/j.scitotenv.2020.140552
- Yang, W., Chen, M., Zheng, M., He, Z., Zhang, X., Qiu, Y., et al. (2015). Influence of a Decaying Cyclonic Eddy on Biogenic Silica and Particulate Organic Carbon in the Tropical South China Sea Based on ^{234}Th - ^{238}U Disequilibrium. *PloS One* 10 (8), e0136948. doi: 10.1371/journal.pone.0136948
- Zhang, J., Li, H., Xuan, J., Wu, Z., Yang, Z., Wiesner, M. G., et al. (2019). Enhancement of Mesopelagic Sinking Particle Fluxes Due to Upwelling, Aerosol Deposition, and Monsoonal Influences in the Northwestern South China Sea. *J. Geophys. Res.* 124 (1), 99–112. doi: 10.1029/2018JC014704
- Zhuang, Y., Jin, H., Cai, W. J., Li, H., Jin, M., Qi, D., et al. (2021a). Freshening Leads to a Three-Decade Trend of Declining Nutrients in the Western Arctic Ocean. *Environ. Res. Lett.* 16 (5), 054047. doi: 10.1088/1748-9326/abf58b
- Zhuang, Y., Jin, H., Chen, J., Li, H., Ji, Z., Bai, Y., et al. (2018). Nutrient and Phytoplankton Dynamics Driven by the Beaufort Gyre in the Western Arctic Ocean During the Period 2008–2014. *Deep-Sea. Res. Pt. I.* 137, 30–37. doi: 10.1016/j.dsr.2018.05.002
- Zhuang, Y., Jin, H., Chen, J., Ren, J., Zhang, Y., Lan, M., et al. (2020). Phytoplankton Community Structure at Subsurface Chlorophyll Maxima on the Western Arctic Shelf: Patterns, Causes, and Ecological Importance. *J. Geophys. Res.* 125 (6), e2019JG005570. doi: 10.1029/2019JG005570
- Zhuang, Y., Jin, H., Zhang, Y., Li, H., Zhang, T., Li, Y., et al. (2021b). Incursion of Alaska Coastal Water as a Mechanism Promoting Small Phytoplankton in the Western Arctic Ocean. *Prog. Oceanogr.* 197, 102639. doi: 10.1016/j.pocean.2021.102639

Conflict of Interest: The authors declare that the research was conducted in the absence of any commercial or financial relationships that could be construed as a potential conflict of interest.

Publisher's Note: All claims expressed in this article are solely those of the authors and do not necessarily represent those of their affiliated organizations, or those of the publisher, the editors and the reviewers. Any product that may be evaluated in this article, or claim that may be made by its manufacturer, is not guaranteed or endorsed by the publisher.

Copyright © 2022 Yu, Zhuang, Cai and Qi. This is an open-access article distributed under the terms of the Creative Commons Attribution License (CC BY). The use, distribution or reproduction in other forums is permitted, provided the original author(s) and the copyright owner(s) are credited and that the original publication in this journal is cited, in accordance with accepted academic practice. No use, distribution or reproduction is permitted which does not comply with these terms.